Transient ultrahigh gains as a diagnostic in short-pulse heated selenium plasmas

K. G. Whitney, A. Dasgupta, and P. E. Pulsifer
Plasma Physics Division, Naval Research Laboratory, Washington D.C. 20375
(Received 22 March 1994; revised manuscript received 24 April 1994)

The influence of intense picosecond heating and time-dependent ionization on the population dynamics of Ne-like selenium is investigated. We find that highly nonequilibrium plasma conditions and a large gain coefficient $>500\ \mathrm{cm}^{-1}$ can be generated for the $J=0-1$ line at 182 Å at KrF laser intensities $>3\times10^{16}\ \mathrm{W/cm}^2$. Thus, the observation of x-ray lasing at or near the critical surface of a KrF short-pulse, laser heated plasma appears feasible. Its observation would provide important tests of theoretical models for laser absorption, heat conductivity, ion heating, transient ionization, and x-ray laser pumping. The calculations in this paper help to define the minimum intensities and energies of the KrF laser that would be needed to carry out these x-ray amplification experiments using 2 ps full width at $1/e$ maximum pulses. The emission pattern of the amplified x rays would also provide useful diagnostics for the gradient and velocity structure of the blowoff plasma near the critical surface.

PACS number(s): 52.50.Jm, 52.40.Nk, 52.25.Jm, 42.55.Vc

I. INTRODUCTION

Early in their development, it was conjectured that high power, picosecond-pulsed lasers could become useful table-top drivers for x-ray lasers [1]. A number of different schemes for generating population inversions in the plasmas heated by picosecond or subpicosecond lasers were then proposed [2,3]. In this paper, we present the results of calculations that demonstrate the feasibility of generating large transient population inversions within the neonlike ionization stage of selenium using short-pulse picosecond lasers. These inversions are large enough to produce, in principle, a saturated amplified spontaneous emission (ASE) from a plasma <1 mm in length. However, our purpose is not to propose the use of short-pulse lasers to produce a well collimated, bright source of coherent x rays, but rather to propose the use of ASE x rays as a potentially rich source of diagnostic information on laser-matter interactions and short-pulse laser-driven plasma dynamics.

The calculations of this paper show that ASE experiments could be carried out with 1 to 10 picosecond KrF laser pulses heating a preformed selenium plasma at or near the critical surface. The use of selenium has two advantages. One, neonlike selenium x-ray lasers have already been operated in long-pulse (~500 ps) laser-generated plasmas, [4] and a number of their properties have been well studied experimentally [5,6]. Two, fairly comprehensive atomic models of their population dynamics have been constructed and benchmarked against experimental observations [7,8]; one [8] is used in obtaining the calculational results described in this paper.

Ultrashort laser-generated plasmas are also of general interest as picosecond-pulsed sources of kilovolt x rays [9]. Experimental observations clearly indicate the need to rapidly heat a preformed plasma in order to maximize x-ray output. The calculations we present support this observation.

Specifically, lasing has both been seen and predicted in two $J=0-1$ and two $J=2-1$ $3p$ to $3s$ transitions in neonlike selenium [7,10] at an ion density of $\sim2\times10^{19}\ \mathrm{cm}^{-3}$. However, at higher densities corresponding roughly to the underlying ion densities near the critical surface of a KrF laser-produced selenium plasma, our calculations show that the $J=2-1$ transitions cannot be inverted and show no gain even in transient ionization. The $J=0$, $3p$ states, on the other hand, are strongly populated from both the ground state and from the $J=1$, $3d$ states due to the large monopole and dipole excitation rates from the ground state to the $J=0$, $3p$ and $J=1$, $3d$ states, respectively. Hence, during transient excitation, a large population inversion is established between the $J=0$, $3p$ and $J=1$, $3s$ states at plasma densities corresponding to the KrF critical surface. This statement is less true by an order of magnitude for a plasma in collisional-radiative equilibrium at the same densities.

This paper is structured as follows. In Sec. II, a brief description is given of the ionization calculation and of the atomic model used. These model calculations focus on the local ionization dynamics of a small plasma volume element and ignore motional hydrodynamics effects. Of interest are the degrees of ionization and $3p$-$3s$ population inversion that can be achieved as a function of the local laser intensity driving the local heating of the plasma. These results are described in Sec. III. They suggest that a short-pulse KrF laser should be capable of generating large population inversions between the $J=1$, $3s$ and the $J=0$, $3p$ states of Ne-like selenium and transient ASE outputs. Finally, in Sec. IV, the use of these amplified x-ray outputs to diagnose short-pulse experiments is discussed.

II. THE MODEL

Because the hydrodynamic expansion of a blowoff plasma generally occurs on the order of nanosecond time scales, the picosecond heating and ionization of a preformed selenium plasma can initially be studied by ignor-

ing the effects of hydrodynamic expansion. The ability to freeze the hydrodynamics to first approximation was one of the early motivations for doing short-pulse experiments. For this purpose, we utilized the hot-spot model described earlier [11] to determine the ionization response of selenium to picosecond heating. The selenium atomic model in the present calculation consists of the hydrogenic lumped-state model described in Ref. [12], to which the neonlike and fluorinelike structure, which is described in Ref. [8], was added. This combined model provides a full description of the transient excitation and ionization of all ionization stages as well as all 26 $n=3$ states in the neonlike stage from which x-ray lasing has been observed.

In the hot-spot model, the following coupled equations are solved:

$$\frac{dN_\mu}{dt}=\sum_\nu W_{\mu\nu}(N_e,T_e)N_\nu,\quad \mu=1,\ldots,n \tag{1}$$

$$N_e=\sum_\mu Z_\mu N_\mu,\quad E_i=\sum_\mu E_\mu N_\mu\ , \tag{2}$$

$$\frac{d}{dt}(\tfrac{3}{2}N_e kT_e+E_i)=S_e-Q_h-R_i -R_{\text{brems}}-\frac{3m_e}{m_i}\frac{N_e k}{\tau_e}(T_e-T_i)\ , \tag{3}$$

$$\frac{d}{dt}(\tfrac{3}{2}N_i kT_i)=\frac{3m_e}{m_i}\frac{N_e k}{\tau_e}(T_e-T_i)\ , \tag{4}$$

where S_e represents the laser energy absorption rate per unit volume, and Q_h is a phenomenological representation of the heat conduction losses that might occur from the tight focus of a laser-heated plasma. The selenium model contains $n=189$ states and population densities, $\{N_\mu\}$. $\{Z_\mu\}$ and $\{E_\mu\}$ are the ionic charges and energies of these states. They are coupled by the complete set of collisional ionizations and excitations and radiative and collisional decays, $\{W_{\mu\nu}\}$, described in Refs. [8] and [12]. The energy equation, $dE_i/dt=Q_i-R_i$, is derived from Eq. (1). R_i is the sum of the optically thin line and free-bound radiation loss rates, which are obtained from the radiation terms in the rate equations [Eqs. (1)] Q_i is the rate of inelastic collisional energy transfer from the electrons to the ions. R_{brems} is the rate of bremsstrahlung losses from the plasma. In picosecond-heated plasmas, both R_i and R_{brems} are negligible relative to S_e, Q_h. The rate of thermal energy transfer from the electrons to the ions, given by the last term on the right-hand side of Eq. (3), is proportional to T_e-T_i. The expression for this term is taken from Braginskii [13]. It is inversely proportional to the electron-ion collision time τ_e.

The expression for Q_h, taken from Ref. [11], like S_e, is proportional to τ_e. Q_h is also determined in terms of a free parameter, the electron temperature gradient scale length, l_e. This scale length can be arbitrarily chosen to allow one to estimate the maximum effect of heat losses on the time history of the electron temperature, T_e. These losses are averaged over the volume of an absorption sphere, i.e., a sphere whose radius, r, is roughly of the order of the inverse bremsstrahlung absorption length of the laser radiation near the critical surface. Thus, the expression for Q_h used in these calculations is

$$Q_h=\frac{3\kappa_e T_e}{rl_e}\cong 12.0\frac{N_e kT_e}{m_e}\tau_e\frac{3kT_e}{rl_e}\ , \tag{5}$$

whenever Q_h is less than a free streaming limit, $Q_h^{\text{fs}}=0.3N_e kT_e v_{\text{th}}$, where $v_{\text{th}}\equiv\sqrt{2kT_e/m_e}$. Otherwise, Q_h is set equal to Q_h^{fs}.

We consider the physical situation in which a prepulse is used to generate a small blowoff plasma containing ion densities that are needed to produce a critical surface corresponding to the 0.25 μm wavelength of a KrF laser. The critical surface electron density of a 0.25 μm wavelength laser is $N_e^c=1.8\times10^{22}$ cm^{-3}. The main KrF pulse can then be used to resonantly heat and ionize selenium near this surface where the ion density is $\leq 7\times10^{20}$, i.e., at this ion density, selenium can be 26 times ionized before the critical electron density is reached. At 7×10^{20} ions/cm^3, the gains of the $J=0$–1 and $J=2$–1 lines at 1 keV would be either small or zero, if the plasma were in collisional-radiative equilibrium (CRE) [8]. We assume that the blowoff plasma has a sufficiently small scale length that a substantial portion of the main laser pulse can be deposited at or near this critical surface by resonant inverse bremsstrahlung [14]. Laser absorption then occurs at a rate given by $S_e(t)=\kappa_L(t)I_L(t)$, where I_L is the incident laser intensity and κ_L is the absorption coefficient given, from Refs. [11] and [14], by

$$\frac{1}{\kappa_L}=\frac{8.3\times10^9 T_e^{3/2}(1-N_e/N_e^c)^{1/2}}{(N_e^2/N_i)\ln\Lambda(N_e/N_e^c)}\ . \tag{6}$$

In this expression, $\ln\Lambda$ is the Coulomb logarithm.

Equations (1)–(6) describe inverse bremsstrahlung, resonant heating at or near the critical surface of a small volume element of plasma whose electrons are cooled by both electron-ion elastic and inelastic collisions and, phenomenologically, by (potentially large) flux limited, heat conduction energy losses. The volume element used in our calculations has a fixed ion density of approximately 6×10^{20} and a fixed radius of 10 μm, which is of the order of the laser absorption length. This volume element is heated with a KrF laser pulse of 2 ps full width at $1/e$ maximum.

III. RESULTS

Figures 1 and 2 show a typical response of the plasma temperature and ionization, respectively, to a Gaussian laser pulse of peak intensity, $I_L^{\max}=2\times10^{15}$ W/cm^2. In order to illustrate the rapidity of the ionization, we began these calculations with a cold ($\sim$2 eV) weakly ionized plasma. The laser pulse peaks at 3 ps and the scale length for heat conduction losses was initially taken to be 100 μm [11] so that heat losses remain nonflux limited throughout the calculation. (They approached the flux limit in the highest laser intensity calculation described below but, in all cases described in this paper, the calculations were not flux limited.)

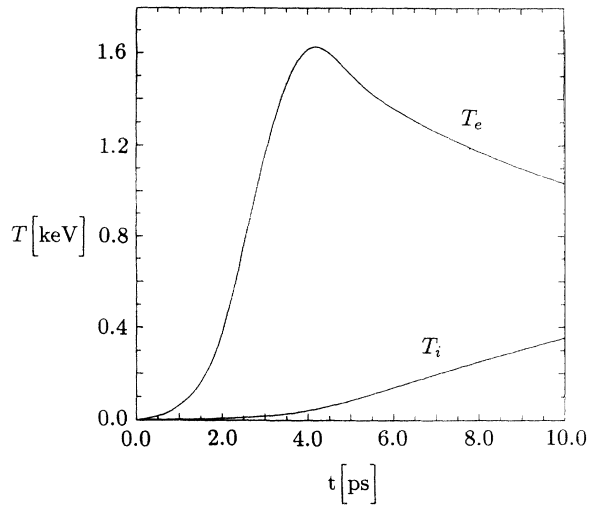

FIG. 1. Calculated electron (T_e) and ion (T_i) temperatures vs time for $I_L^{\max}=2\times10^{15}$ W/cm^2.

Because moderate heat losses were simulated in this calculation, the electron temperature, which had a peak above 1600 eV at 4 ps, fell to only 1030 eV at 10 ps. The rise in the ion temperature as well as the rapid ionization, which reached the neonlike ionization stage in 5.5 ps (Fig. 2), also contributed to the cooling of the electrons, but to a lesser degree. However, in spite of this cooling, the plasma continued to ionize over the entire 10 ps interval because the rise in ionization lags the rise in T_e and because T_e reaches such a large peak. In other words, at $T_e=1030$ eV, the plasma will ionize beyond the Ne-like ionization stage. However, subsequent ionization is slowed by the much larger excitation energies of the L shell compared to the M shell. At 6×10^{20} ions/cm^3, therefore, selenium is an ideal candidate material for generating population inversions within the Ne-like ionization stage on a 10 ps time scale.

Because the ion temperature is low, Doppler broadening is only a small correction to the collisional broadening of the lasing lines. Therefore, Voigt profiles were needed to compute the gains, g, of the $J=0-1$ lines at line center [15].

$$g=\frac{A\lambda^2}{8\pi\Delta\nu_V}\left[N_u-\frac{g_u}{g_l}N_l\right], \tag{7}$$

where A is the radiative decay rate for the transition, λ is the wavelength, and $\{N_u,g_u\}$, $\{N_l,g_l\}$ are the populations and degeneracy factors of the upper and lower states of the transition, respectively. To determine the Voigt profile at line center, $1/\Delta\nu_V$, we used an expression derived by Apruzese [16].

$$\frac{1}{\Delta\nu_V}\cong\frac{1+a}{1+1.88a+1.772a^2}\frac{1}{\sqrt{\pi}\Delta\nu_D}, \tag{8}$$

where $\Delta\nu_D=\sqrt{2kT_i/(m_ic^2)}(c/\lambda)$ is the Doppler linewidth and $a\equiv\Gamma_T/(4\pi\Delta\nu_D)$ is the Voigt parameter. Γ_T is the sum of the inverse lifetimes (radiative plus collisional) of the upper and lower states. In our atomic model, these linewidths are approximately 100 mÅ for both $J=0-1$ lines. Moreover, the calculated $J=2-1$ linewidths were roughly 1.5 times larger than those of the $J=0-1$ lines. These results compare favorably to recent experiments [6], in which a 50 mÅ linewidth was measured for the $J=2-1$ line at 206 Å. Furthermore, it was speculated that collisional effects were playing a significant role in determining the line profile.

In the calculation under discussion (see Figs. 1 and 2), the gains of the two $J=0-1$ lines acquired nonzero values after 4 ps, and they peaked at 5.5 ps. Then, they steadily fell to roughly one-third of their peak values at 10 ps. This behavior is displayed in Fig. 3.

As the maximum laser intensity $I_L^{\max}$ of the 2 ps pulses was varied, the size of the $J=0-1$ population inversions increased as the amount of laser energy deposited in the plasma increased. This behavior is shown in Fig. 4. At

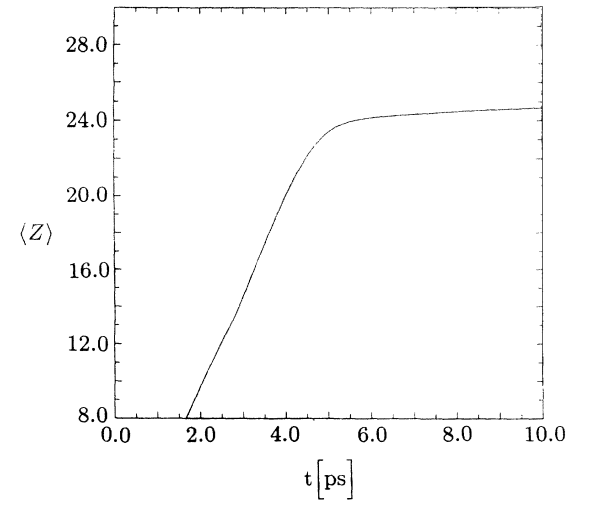

FIG. 2. Calculated average charge state $\langle Z\rangle\equiv N_e/N_i$ vs time for $I_L^{\max}=2\times10^{15}$ W/cm^2.

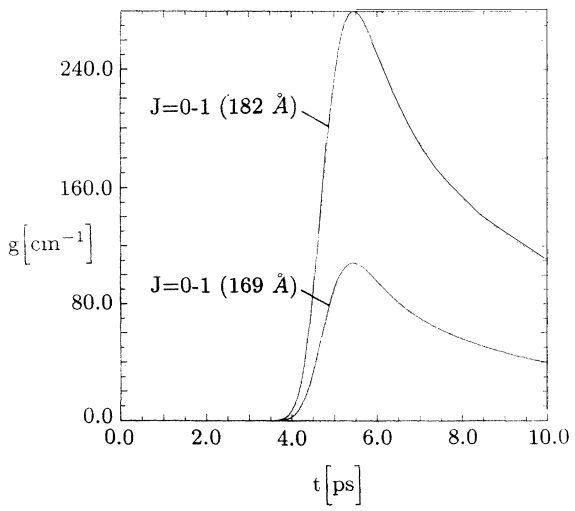

FIG. 3. Calculated gains for the two $J=0-1$, $3s-3p$ transitions vs time for $I_L^{\max}=2\times10^{15}$ W/cm^2.

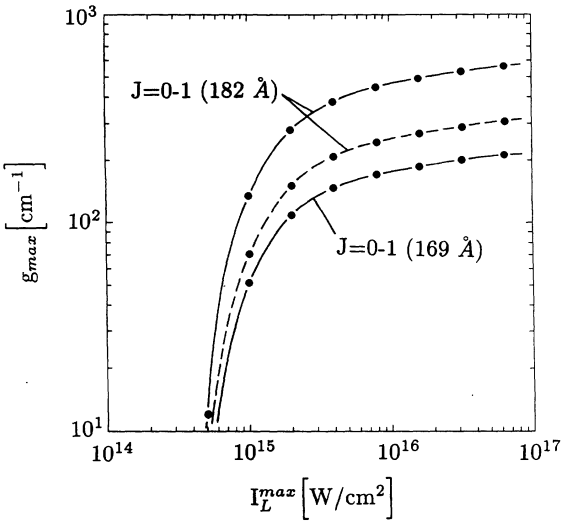

FIG. 4. Calculated maximum gains for the two $J=0-1$, $3s-3p$ transitions vs the maximum KrF laser intensity. The solid $J=0-1$ (182 Å) curve corresponds to no modification of the $J=0$ monopole excitation rate, and the dashed curve, to a factor of 2 reduction of this rate.

$I_L^{max}=2\times10^{15}$, corresponding to Figs. 1 and 2, the maximum gain, g_{max}, of the 182 Å $J=0-1$ line was 280 cm^{-1}, while the $J=0-1$ line at 169 Å achieved a maximum gain of 108 cm^{-1}. However, g_{max} continued to rise as I_L^{max} was increased. At intensities larger than 6×10^{16} W/cm^2, the 182 Å line is predicted to reach gains in excess of 550 cm^{-1}. The full width at half maximum of the ASE pulses that would be generated in these plasmas is approximately 4 ps (see Fig. 3). Note that the propagation distance of a 4 ps x-ray pulse within an amplifying medium is 1.2 mm.

One problem associated with the neonlike selenium gain models that have been constructed to date is that they predict the largest gain for the $J=0-1$ line at 182 Å. In long pulse x-ray laser experiments, however, larger gains were measured for the $J=2-1$ lines. This problem was discussed in Ref. [8], where it was noted that a factor of 2 decrease in the magnitude of the calculated monopole excitation cross section, which couples the neonlike ground state to the (upper) $3p$ state of this 182 Å transition, was sufficient to reverse the relative magnitudes of the $J=0-1$ and $J=2-1$ gains in CRE at an ion density of $\sim10^{19}$. The effect of this cross-section reduction on the short-pulse gain calculations is shown by the dashed curve in Fig. 4. This reduction in the monopole rate produced less than a factor of 2 reduction in the peak gain of the 182 Å line because this line is strongly populated by the uppermost of the $J=1$, $3d$ states. Moreover, this rate reduction did not significantly change the gain of the 169 Å line.

Two factors combine to produce the large gains seen in Fig. 4. One, the calculations are carried out at an ion density an order of magnitude larger than the densities of the gain medium inferred in the long-pulse x-ray laser experiments. Thus, collisional excitation rates are also an order of magnitude larger, enhancing both the $3p$, $J=0$ upper laser levels and the $3d$ states that feed them. Two, the plasma ionizes through a succession of nonequilibrium states. Hence, by the time neonlike ground states are plentiful, the electrons are already hot enough to ionize the plasma into the higher ionization stages of the L shell, well beyond the neonlike stage. Under these conditions, unlike those found in CRE plasmas, the exponential temperature dependence of the ground state excitation rates has been eliminated, and, consequently, these rates are much larger than they would be in CRE. An added feature of this enhanced pumping shows up with the $3d$ states. The two $3d$ states that feed the $J=0$, $3p$ states are suppressed in CRE relative to the other metastable $3d$ states because of strong radiative decays to the ground state. The opposite is true during transient ionization, i.e., strong radiative decays imply that the collisional excitation rates of these $3d$ states are also strong. (In our calculations, they are roughly one to two orders of magnitude larger than the excitation rates to the other ten metastable $3d$ states.) Thus, the two $3d$ states that strongly couple to the $3p$, $J=0$ states become relatively overpopulated, rather than underpopulated, during transient ionization since the other $3d$ states do not have the time to equilibriate with them. Because of the high electron temperatures, the role of the $3d$ states in populating the $J=0$, $3p$ states is significantly enhanced in these transient calculations compared to CRE calculations.

Figures 1–4 define the pulsewidth and intensity requirements for the short-pulse laser that would be needed to carry out the above x-ray laser experiments. The energy requirements of the laser can be estimated as follows. The amount of absorbed energy per unit mass will rise with I_L^{max}. For example, Fig. 5 shows the amount of energy per unit mass absorbed in each of the above calculations. A cylinder that is 10 μm in radius and 0.1 mm in length with 6×10^{20} ions/cm^3 contains 2.5×10^{-3} μg of selenium. Thus, heating this cylinder with a 2 ps laser pulse at 3×10^{16} W/cm^2 would require 1.4 J of energy (570 J/μg$\times2.5\times10^{-3}$ μg). In addition to this energy, one must add the laser energy absorbed in other portions

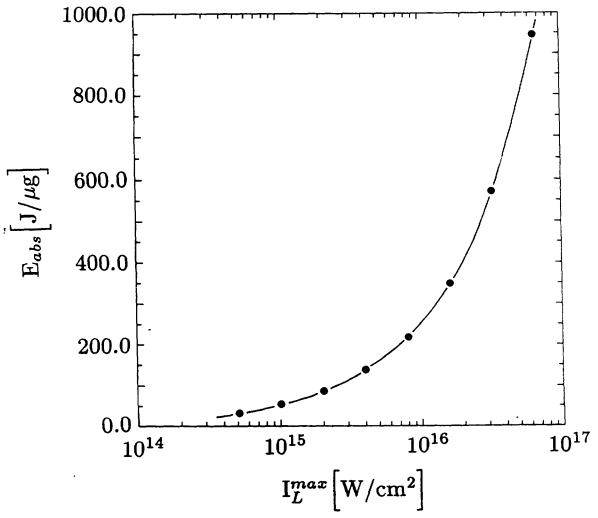

FIG. 5. Calculated total laser energy absorbed per microgram of selenium as a function of the maximum KrF laser intensity.

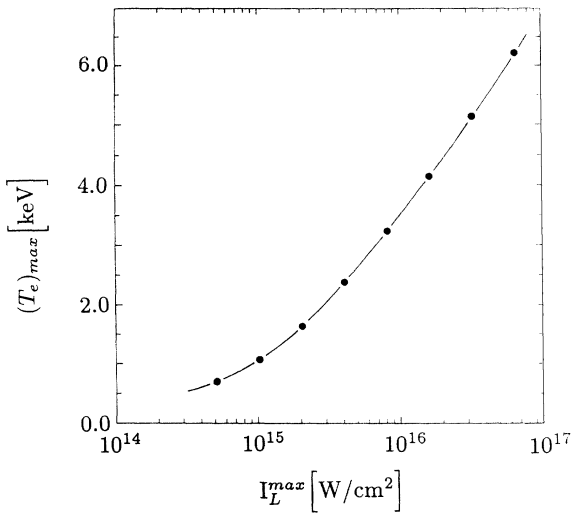

FIG. 6. Calculated maximum electron temperature as a function of the maximum KrF laser intensity.

of the blowoff plasma as well as reflected energy.

The calculated peaks of the electron temperature, which are shown in Fig. 6 as a function of $I_L^{\max}$, are correlated to the absorbed laser energy. Whether one models the laser absorption process by resonant inverse bremsstrahlung or by resonance absorption will not alter the main results of this paper, i.e., they will not alter the correlation of the peak plasma temperature to the absorbed laser energy to the laser incident intensity. The fraction of incident laser energy that is absorbed is a known or measurable quantity. What the calculations of this paper show is the effect of physically realizable amounts of rapid laser energy deposition on the ionization dynamics of a selenium plasma assuming non-flux-limited energy losses from the x-ray laser volume during the emission of the ASE pulse.

IV. DISCUSSION AND CONCLUSIONS

We have investigated the feasibility of producing ASE from Ne-like selenium through the use of high-intensity ($>10^{15}$ W cm^{-2}), short-pulse (2 ps), KrF lasers. Our calculations show that a large gain coefficient can be generated for the $J=0-1$ line at 182 Å, when the laser intensity exceeds 10^{16} W cm^{-2}. Below this level, the gain becomes a sensitive function of laser intensity. These results are based on a comprehensive atomic model that has been favorably compared with experiment. The plasma is modeled with the hot spot model [11], which provides reasonable estimates of all the important heating and cooling processes on the picosecond timescale of the laser pulse.

In an actual experiment, we might expect each of these processes to be affected by factors not included in the hot-spot model. These factors, if present, would also significantly affect any detailed hydrodynamic modeling of the plasma. For example, at the laser intensities used in these calculations, non-Maxwellian electron distributions will be generated [17–19]. At any given level of ionization, these distributions will enhance the rates for exciting the plasma, and they are expected to generate larger population inversions than were attained for the gains shown in Fig. 4. Hence, there is reason to believe that the gains shown in Fig. 4 are smaller than may be achievable in an actual short-pulse KrF experiment. Another effect of the non-Maxwellian distributions is to alter the values of κ_L, κ_e, and τ_e that are used in the hot-spot calculations. For example, Langdon [17] calculated a factor of $\cong 2$ reduction in κ_L due to laser-generated non-Maxwellian distributions. Thus, these distributions are expected to shift the curves in Fig. 4 both upwards and sideways.

The effects of generating an ion-acoustic turbulence at the critical surface can also significantly affect the gains in Fig. 4. Some of the more important effects might be modeled through the use of a single parameter, β [19] which modifies a number of important plasma properties. For example, laser absorption would be increased, $\kappa_L^{ia}=\kappa_L(1+\beta)$, and the electron-ion collision time, $\tau_e^{\text{eff}}\equiv\tau_e/(1+\beta)$, would be reduced, leading to inhibited electron heat flow, $Q_h^{\text{eff}}\equiv Q_h/(1+\beta)$, and increased coupling between the electron and ion thermal energies [see Eq. (4)]. Higher ion temperatures would increase the Doppler broadening and somewhat lower the gains that would be calculated at line center under fairly mild levels of saturated ion-acoustic turbulence. However, determining the levels of microturbulence that can actually be generated in short-pulse experiments is a problem currently under investigation [20].

Thus, when either a non-Maxwellian electron distribution or plasma microturbulence is generated by the laser absorption processes, the hydrodynamics that is needed to model short-pulse experiments will be significantly modified. It is not unreasonable, therefore, to ignore hydrodynamic expansion initially, as the hot-spot model does, when investigating the feasibility of generating ASE in short-pulse laser-heated or laser-produced plasmas. Depending on the energy contained in the KrF pulse, its deposition profile, and on the amount of x-ray refraction, photons emitted in all directions by the inverted populations would receive varying amounts of amplification [21]. If the expansion of the blowoff plasma has velocity gradients that significantly Doppler shift the emission profile of the x rays that travel in the direction of the expansion, their amplification could be affected and reduced. In this case, the emission pattern of the ASE might contain useful information about the velocity profile of the expansion.

The emission pattern of the ASE could also contain information on density gradients in the gain region because of x-ray refraction. In earlier selenium, x-ray laser experiments, it was estimated that the transverse density gradient scale length, L_d^{LP}, was 100 μm and that the 200 Å x rays traveled a distance, L_z^{LP}, of 1 cm in an electron density, N_e^{LP}, of 5×10^{20} cm^{-3} before being refracted out of the amplifying region [10]. These experiments were carried out in plasmas that were 1 to 4 cm in length. Refraction was observed to play an important role in the experiments, but it did not nullify the amplification. An estimate for the distance, L_z^{SP}, that a 200 Å photon would

travel in a short-pulse experiment before refracting out of a region defined by an electron density, N_e^{SP}, and a transverse density scale length, L_d^{SP}, can be made from [10]

$$\frac{L_z^{SP}}{L_z^{LP}} = \frac{L_d^{SP}}{L_d^{LP}} \left[\frac{N_e^{LP}}{N_e^{SP}} \right]^{1/2} . \quad (9)$$

If we assume that $L_d^{SP} \cong 10\ \mu m$ and that $N_e^{SP} \cong 10^{22}\ cm^{-3}$, then Eq. (9) implies $L_z^{SP} \cong 0.1$ mm. If somewhat longer length plasmas than this are needed to see several e foldings of amplification, refraction of the amplified x rays will provide an important density gradient diagnostic in these experiments.

Because x-ray laser performance is potentially a sensitive measure of underlying plasma conditions, the observation of x-ray lasing in short-pulse experiments would provide important tests of the theoretical models that are used to describe laser absorption, heat conduction, ion heating, transient ionization, and x-ray laser pumping. Since the peak of the electron temperature as a function of I_L^{max} is correlated to the absorbed laser energy and the amount of heat conduction, the simultaneous measurement of this temperature along with the $J=0-1$ gains would provide useful information on the presence and influence of microturbulence and non-Maxwellian electron distributions on underlying critical surface phenomena.

ACKNOWLEDGMENTS

This work was sponsored by the Ballistic Missile Defense Office/DFI. The authors would like to thank J. P. Apruzese for his helpful comments and for the use of his Voigt profile formula.

[1] K. Boyer and C. K. Rhodes, in *Southwest Conference on Optics,* edited by R. S. McDowell, SPIE Proc. Vol. 540 (SPIE, Albuquerque, NM, 1985), pp. 196–204.
[2] See, for example, *Femtosecond to Nanosecond High-Intensity Lasers and Applications,* edited by E. M. Campbell, SPIE Proc. Vol 1229 (SPIE, Bellingham, WA, 1990).
[3] P. Amendt *et al.*, Phys. Rev. Lett. **66**, 2589 (1991).
[4] D. L. Matthews *et al.*, Phys. Rev. Lett. **54**, 110 (1985).
[5] M. D. Rosen *et al.*, Phys. Rev. Lett. **59**, 2283 (1987).
[6] J. A. Koch *et al.*, Phys. Rev. Lett. **68**, 3291 (1992).
[7] R. A. London *et al.*, J. Phys. B **22**, 3363 (1989).
[8] A. Dasgupta *et al.*, Phys. Rev. A **46**, 5973 (1992).
[9] M. M. Murnane *et al.*, Science **251**, 531 (1991); J. A. Cobble *et al.*, Phys. Rev. A **39**, 454 (1989); H. M. Milchberg *et al.*, Phys. Rev. Lett. **67**, 2654 (1991); J. P. Apruzese, Phys. Rev. E **47**, 2798 (1993).
[10] C. J. Keane *et al.*, J. Phys. B **22**, 3343 (1989).
[11] K. G. Whitney and J. Davis, J. Appl. Phys. **45**, 5294, (1974).
[12] K. G. Whitney and M. C. Coulter, IEEE Trans. Plasma Sci. **16**, 552 (1988).
[13] S. I. Braginskii, *Reviews of Plasma Physics,* edited by M. A. Leontovich (Consultants Bureau, New York, 1965), p. 205.
[14] T. W. Johnston and J. M. Dawson, Phys. Fluids **16**, 722 (1973).
[15] R. C. Elton, *X-ray Lasers* (Academic, San Diego, 1990), p. 22.
[16] J. P. Apruzese, private communication.
[17] A. B. Langdon, Phys. Rev. Lett. **44**, 575 (1980).
[18] P. Alaterre *et al.*, Phys. Rev. A **34**, 1578 (1986).
[19] K. G. Whitney and P. E. Pulsifer, Phys. Rev. E **47**, 1968 (1993).
[20] S. C. Wilks *et al.*, Phys. Rev. Lett. **69**, 1383 (1992).
[21] K. G. Whitney, J. Davis, and J. P. Apruzese, *Cooperative Effects in Matter and Radiation,* edited by C. M. Bowden, D. W. Howgate, and H. R. Robl (Plenum, New York, 1977), p. 115.